

c-Axis Penetration Depth of Hg-1201 Single Crystals

J. R. Kirtley

IBM T. J. Watson Research Center, P.O. Box 218, Yorktown Heights, New York 10598

K. A. Moler*

Department of Physics, Princeton University, Princeton, New Jersey 08544

G. Villard and A. Maignan

CRISMAT-ISMRA, 6 Boulevard du Maréchal Juin, 14050 Caen Cedex, France

(Received 13 March 1998; revised manuscript received 13 July 1998)

We have magnetically imaged interlayer Josephson vortices emerging from an *ac* face of single crystals of the single layer cuprate high- T_c superconductor (Hg, Cu)Ba₂CuO_{4+ δ} . These images provide a direct measurement of the *c*-axis penetration depth, $\lambda_c \sim 8 \mu\text{m}$. This length is a factor of 8 longer than predicted by the interlayer tunneling model for the mechanism of superconductivity in layered compounds, indicating that the condensation energy available through this mechanism is 50 times smaller than is required for superconductivity. [S0031-9007(98)07101-4]

PACS numbers: 74.72.-h, 73.40.Gk, 73.40.Rw, 74.50.+r

In the interlayer tunneling (ILT) model for superconductivity in layered superconductors such as the cuprates [1–4], transport of carriers between the planes is incoherent in the normal state, but coherent interlayer transport is allowed for Cooper pairs. The coherent pair tunneling lowers the *c*-axis kinetic energy, supplying the superconducting condensation energy, E_c . Anderson [4,5], Leggett [6,7], and Chakravarty [8] have each argued that the comparison of the experimentally measured *c*-axis penetration depth, λ_c , and the value determined within the ILT model from the condensation energy, λ_{ILT} , is an important test of the ILT mechanism. In all presently published versions of the theory, $\lambda_c \approx \lambda_{\text{ILT}}$.

The calculation of λ_{ILT} and its comparison with experiment are most straightforward in materials with a single copper oxide layer per unit cell, such as La_{2- x} Sr _{x} CuO_{4+ δ} ($\lambda_{\text{ILT}} \approx 3 \mu\text{m}$ [5]), HgBa₂CuO_{4+ δ} ($\lambda_{\text{ILT}} \approx 1 \mu\text{m}$ [5]), and Tl₂Ba₂CuO_{6+ δ} ($\lambda_{\text{ILT}} \approx 1 \mu\text{m}$ [5]). In La_{2- x} Sr _{x} CuO_{4+ δ} (La-214), measurements of the Josephson plasma frequency $\omega_p = c\lambda_c^{-1}\epsilon^{-1/2}$ (where c is the speed of light and ϵ is the dielectric constant of the interlayer medium) [9,10] are in good agreement with the predictions of the ILT model [5]. In Tl₂Ba₂CuO_{6+ δ} (Tl-2201), Moler *et al.* observed interlayer Josephson vortices with $\lambda_c = 17\text{--}21$ microns [11], in disagreement with λ_{ILT} . Measurements of the plasma resonance ω_p and dielectric constant ϵ by Tsvetkov *et al.* also indicate $\lambda_c = 17 \mu\text{m}$ [10,12]. In HgBa₂CuO_{4+ δ} (Hg-1201), Panagopoulos *et al.* obtained a value of $\lambda_c(T=0) = 1.36 \pm 0.16 \mu\text{m}$ from magnetic susceptibility data on oriented powders [13]. It has been suggested that Tl-2201 is anomalous, perhaps due to crystalline defects that make it not a true single-layer material [5]. Therefore, as both Anderson [5] and Leggett [7] have pointed out, a confirmation of the *c*-axis penetration depth in Hg-1201 seems essential to resolving this issue.

In this Letter we directly measure the *c*-axis penetration depth in Hg-1201 by magnetically imaging interlayer Josephson vortices emerging from the *ac* face of single crystals. These measurements give $\lambda_c \approx 8 \mu\text{m}$, much longer than the value $\lambda_c \approx 1 \mu\text{m}$ reported by Panagopoulos *et al.* [13]. Our value for λ_c , when combined with previous results from Tl-2201, make it appear unlikely that presently published versions of the ILT model are the mechanism of superconductivity in the cuprate high- T_c superconductors.

The Hg-1201 crystal growth has been described previously [14]. Our method consists in preparing a Ba/Cu/O precursor in flowing oxygen, and then mixing it with HgO to make a 0.8:2:1.2 ratio of Hg:Ba:Cu. An alumina crucible containing this powder is then sealed in a silica tube. After 48 hours of thermal treatment, black, plateletlike crystals are extracted. The largest crystals (typical dimensions $\sim 1 \times 1 \times 0.08$ mm) are selected for transport and SQUID imaging measurements. EDX and electron diffraction measurements lead to the formula Hg_{0.8}Cu_{0.2} for the mixed mercury layer. The copper position is displaced with respect to the Hg site in the mixed layer as shown from structural refinements. The existence of structural defects would be detrimental to the present work. Two kinds of experiments were made to check the crystal quality. First, *c*-axis misorientation due to stacking faults has been ruled out: Rocking curves on (001) reflections yield a half width at half maximum of about 0.1°, ensuring a *c*-axis dispersion smaller than or equal to this value. Second, high resolution electron microscopy (HREM) shows very regular contrast at the atomic level that demonstrates the lack of intergrowths, extensive defects, or cationic ordering phenomena [15]. Although both x-ray diffraction and HREM techniques are principally sensitive to cations, so that some local oxygen inhomogeneities cannot be ruled out, the amount of such inhomogeneities is

limited by the sharpness of the magnetic superconducting transitions, $\delta T_c(10\% - 90\%) = 3$ K. The Hg-1201 single crystals were mounted in epoxy so that the ac face was aligned vertically, and then the sample and epoxy were polished to make a flat, smooth surface to scan.

The magnetic imaging measurements were made with a scanning SQUID microscope [16], in which a sample is scanned relative to a superconducting pickup loop oriented nearly parallel to the sample surface. The data are represented as the magnetic flux Φ_s through the pickup loop, vs the loop's position in the x, y plane. The pickup loop is fabricated with well-shielded leads to an integrated Nb-Al₂O₃-Nb SQUID. The spatial resolution of the microscope is set by the size of the pickup loop, an octagon $L = 4 \mu\text{m}$ in diameter (half the size of that used in Ref. [11]). The SQUID substrate was polished to within a few microns of the pickup loop, oriented an angle $\theta \sim 20^\circ$ from parallel to the sample, and scanned with the tip touching the sample. Fits to data on Abrikosov vortices indicate that the pickup loop is about $z_0 = 1 \mu\text{m}$

above the surface of the sample under the experimental conditions used here. Our images were made with both sample and SQUID immersed in liquid helium at 4.2 K.

Figure 1 shows a SSM image of a $512 \mu\text{m} \times 256 \mu\text{m}$ area of the crystal and surrounding epoxy, cooled and imaged in a field of about 10 mG. The outer edges of the crystal face are indicated by dashed lines. Visible in this image are about 50 interlayer Josephson vortices. The decay of the observed vortex magnetic flux perpendicular to the layers (along the c axis) is determined by the size of the pickup loop. In contrast, the extent of the images of the vortices along the layers provides a direct measure of λ_c . The positions of the vortices are presumably determined by a combination of the sample cooling conditions and the pinning potential. The edges of the crystal face, consistent with observations on other materials, tend to be free of trapped vortices. Some of the vortices are spaced too closely to be resolved. However, 20 of the most isolated vortices have a 10% standard deviation of the full width at half maximum amplitude of cross sections through them along the plane direction. Although one must consider that the vortices may be pinned in areas with unusually weakly coupled planes,

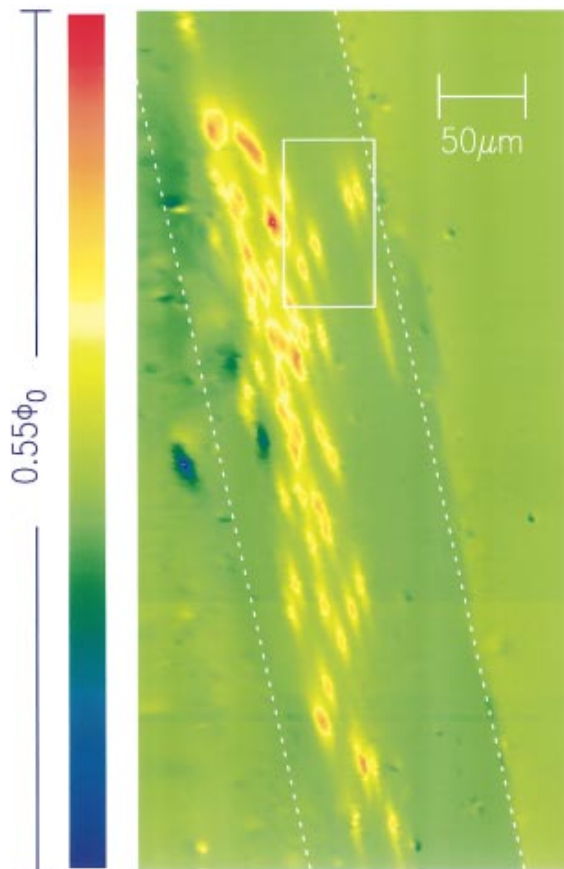


FIG. 1(color). Scanning SQUID microscope image of a 256×512 micron area of the edge of a single crystal of Hg-1201, cooled in a field of about 10 mG, and imaged at 4.2 K. The false color lookup table corresponds to a total variation in flux through the SQUID pickup loop of $0.55\Phi_0$. The dashed lines indicate the top and bottom ab faces of the crystal. The box indicates the area that is expanded in Fig. 2.

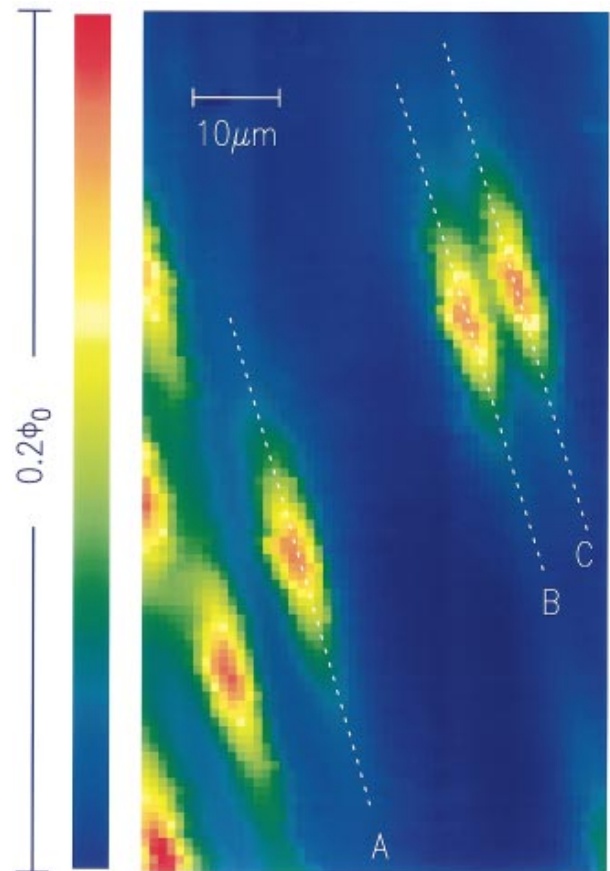


FIG. 2(color). Expanded view of a $54 \times 100 \mu\text{m}$ area of the image of Fig. 1. The dashed lines indicate the paths of cross sections through the data parallel to the planes displayed in Fig. 3.

the uniformity of the vortex shapes over a large area of the crystal face suggests that we are measuring the intrinsic penetration depth. This is supported by the good agreement between bulk plasma resonance measurements of ω_j and local interlayer Josephson vortex imaging measurements of λ_c in Tl-2201 [12].

Three vortices chosen for further analysis are shown in Fig. 2. Cross sections through the image data parallel to the layers are displayed in Fig. 3.

The z component of the magnetic field of an interlayer vortex above the superconducting surface is given by [17]:

$$h_z(\mathbf{r}, z) = - \int \frac{d^2\mathbf{k}}{(2\pi)^2} k \phi(\mathbf{k}) e^{i\mathbf{k}\cdot\mathbf{r} - kz}, \quad (1)$$

where

$$\phi(\mathbf{k}) = - \frac{\phi_0(1 + m_1 k_x^2)}{m_3 \alpha_3 [m_1 k_x^2 \alpha_3 (k + \alpha_1) + k \alpha_3 + k_y^2]}, \quad (2)$$

$\alpha_1 = [(1 + m_1 k^2)/m_1]^{1/2}$, $\alpha_3 = [(1 + m_1 k_x^2 + m_3 k_y^2)/m_3]^{1/2}$, $k = (k_x^2 + k_y^2)^{1/2}$, $m_1 = \lambda_{ab}^2/\lambda^2$, $m_3 = \lambda_c^2/\lambda^2$, $\lambda = (\lambda_{ab}^2 \lambda_c)^{1/3}$, λ_{ab} is the in-plane penetration depth, $\phi_0 = hc/2e$ is the superconducting flux quantum, h is Planck's constant, e is the charge on the electron, x is the distance perpendicular to the planes, and y is the distance parallel to the planes. The fields are summed over the geometry of the pickup loop. Assuming $\lambda_{ab} = 0.17 \mu\text{m}$ [13], this model has two free parameters: λ_c , which determines the length of the vortex, and z_0 , which determines the magnetic amplitude of the vortex image. Fits to the three cross sections (Fig. 3) yield consistent values for the interlayer penetration depth $\lambda_c = 8 \pm 1 \mu\text{m}$.

This measured value is about 8 times longer than the theoretical value in the ILT model: Anderson uses a scaling argument to estimate $\lambda_{ILT} = 1 \pm 0.5 \mu\text{m}$ [5]. The condensation energy for our Hg-1201 single

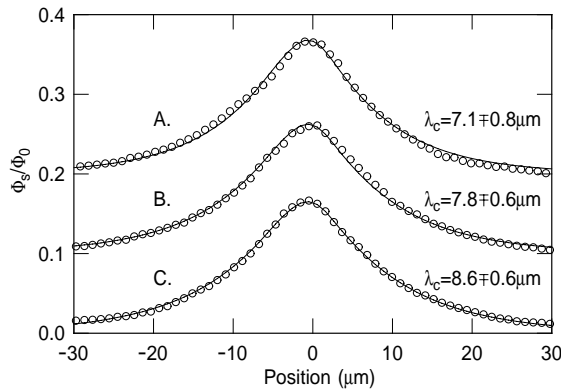


FIG. 3. The symbols are cross-sectional data through the three representative vortices indicated in Fig. 2, offset vertically for clarity. The solid lines are fits to the data, as described in the text. The fit penetration depths λ_c are as labeled in the figure, and the effective heights are $z_0 = 0.66 \pm 0.16 \mu\text{m}$ (A), $0.59 \pm 0.06 \mu\text{m}$ (B), and $0.43 \pm 0.06 \mu\text{m}$ (C). The error bars are assigned using a doubling of the best-fit χ^2 as a criterion.

crystals has been estimated from specific heat measurements to be $E_c = 12-16 \text{ mJ/g}$ [18]. This leads to $\lambda_c = \hbar c / (2ed\sqrt{4\pi E_c}) = 0.95-1.09 \mu\text{m}$, where $d = 0.95 \text{ nm}$ is the interlayer spacing, in good agreement with Anderson's scaling argument. Since the ILT condensation energy is proportional to $1/\lambda_c^2$, the condensation energy which could be supplied by the ILT is at least 50 times smaller than the actual condensation energy in Hg-1201 [5].

A more conventional estimate of λ_c comes from the Lawrence-Doniach model [19]. For diffusive pair transfer (parallel momentum not conserved) between superconducting layers [19-21], the Josephson current between two identical superconducting sheets at $T = 0$ is given by [21] $J_0 = \pi\Delta(0)/2eR_{c,n}$, where $\Delta(0)$ is the zero temperature energy gap and $R_{c,n}$ is the normal state c -axis interplane resistance. The interlayer penetration depth is given by $\lambda_{\perp} = (c\Phi_0/8\pi^2 s J_0)^{1/2}$ [22]. The application of this model requires at least two assumptions: that R_n is temperature independent below T_c , or at least that the temperature dependence can be understood well enough for extrapolation [8], and that the gap is s wave [23-25]. d -wave superconductivity would tend to increase λ_c from this value: in a purely tetragonal d -wave superconductor, with purely diffusive pair transfer, the coupling would be reduced to zero [23-25]. With these considerations in mind, one would not expect the Ambegaoker-Baratoff model to apply quantitatively, but it is, nevertheless, natural to look for a correlation between λ_c and $R_{c,n}$.

Figure 4a shows measurements of the c -axis resistivity of two of our Hg-1201 crystals as a function of temperature. These measurements were made by evaporating four Ag stripes, two on each ab face of the crystal, as diagrammed in the inset of Fig 4a [26]. The contacts as prepared have high resistance, but after an annealing step at 400°C for 10 min the contact resistances drop to 1 to 2 ohms. We have carefully checked that

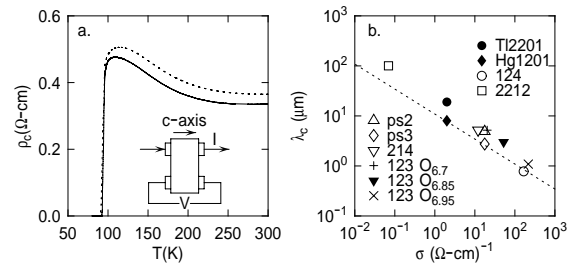


FIG. 4. (a) c -axis resistivity vs temperature for two of our crystals. The contact geometry used is diagrammed in an inset. (b) Correlation plot between c -axis conductivity and c -axis penetration depth, following Basov *et al.* (Ref. [29]). We have included our present data for Hg-1201 and previous data on Tl-1201. The dashed line is the prediction for diffuse tunneling between superconducting layers in an s -wave superconductor assuming a gap value $2\Delta = 28 \text{ meV}$. In this figure 124 = $\text{YBa}_2\text{Cu}_4\text{O}_8$, 2212 = $\text{Bi}_2\text{Sr}_2\text{CaCuO}_8$, ps2 = ps3 = $\text{Pb}_2\text{Sr}_2\text{RCu}_3\text{O}_8$, 214 = $\text{La}_{1.84}\text{Sr}_{0.16}\text{CuO}_4$, 123 = $\text{YBa}_2\text{Cu}_3\text{O}_x$.

such annealing does not alter the superconducting transition by measuring the susceptibility of control crystals before and after such an annealing step. Because of the relatively high anisotropy of Hg-1201 and large thickness of our crystals ($\sim 80 \mu\text{m}$), these crystals are electrically thick [27]. Therefore difficulties in separating the in- and out-of-plane conductivities such as reported by Hussey *et al.* [28] for $\text{YBa}_2\text{Cu}_4\text{O}_8$ should not occur. The midpoint $T_c = 94 \text{ K}$ of the $\rho_c(T)$ curves is consistent with the onset $T_c = 95 - 97 \text{ K}$ observed magnetically on such crystals and confirms that the doping is close to optimal. Taking $\rho_{c,n} = \sigma_{c,n}^{-1} = 0.5 \text{ ohm cm}$, and a BCS gap value $2\Delta = 3.45k_B T_c = 28 \text{ MeV}$, leads to a predicted penetration depth $\lambda_c = (\hbar c^2 / 4\pi^2 \Delta \sigma_{c,n})^{1/2} = 8 \mu\text{m}$ for diffuse pair transfer in an *s*-wave superconductor.

Basov *et al.* [29] have previously noted a correlation between the values of the penetration depth λ_c and the far-infrared *c*-axis conductivity, $\sigma_{c,\text{FIR}}$. In Fig. 4b we add our results for Hg-1201 and Tl-2201 [11], replacing $\sigma_{c,\text{FIR}}$ with $\sigma_{c,n}$ just above T_c . The dashed line is Eq. (2), assuming $2\Delta = 28 \text{ meV}$. This simple model, although it assumes the same Δ for all cuprates, and has the shortcomings outlined above, agrees with all of the measurements to within a factor of 3.

If, as is indicated by our x ray and HREM measurements, the Hg-1201 crystals used in this study, and the Tl-2201 crystals used in the previous study are true single-layer materials, then the long *c*-axis penetration depths $\lambda_c \approx 8 \mu\text{m}$ for Hg-1201 and $\lambda_c \approx 20 \mu\text{m}$ for Tl-2201 pose a serious challenge to the ILT model. Although one can hypothesize structural explanations, perhaps based on the excess copper, to make these results consistent with the ILT model, such explanations must be found for both $(\text{Hg, Cu})\text{Ba}_2\text{CuO}_{4+\delta}$ and $\text{Tl}_2\text{Ba}_2\text{CuO}_{6+\delta}$.

These two results fall into a previously unfilled range of penetration depths in the Basov correlation. This correlation, $\lambda_c \approx (\hbar c^2 / 4\pi^2 \Delta \sigma_{c,n})^{1/2}$, works surprisingly well given the reservations outlined above. It appears that any theoretical description of *c*-axis transport should be consistent with this correlation.

We would like to acknowledge M.B. Ketchen for the design, and M. Bhushan for the fabrication, of the SQUIDS used in our microscope. We would also like to acknowledge useful conversations with P.W. Anderson, S. Chakravarty, A.J. Leggett, C. Panagopoulos, D. van der Marel, V.G. Kogan, and J. Clem.

*Permanent address: Department of Applied Physics, Stanford, CA 94305.

- [1] J. Wheatley, T. Hsu, and P.W. Anderson, *Nature* (London) **333**, 121 (1968).
- [2] P.W. Anderson, *Physica* (Amsterdam) **185C**, 11 (1991); *Phys. Rev. Lett.* **67**, 660 (1991); *Science* **256**, 1526 (1992).
- [3] S. Chakravarty, A. Sudbø, P.W. Anderson, and S. Strong, *Science* **261**, 331 (1993).
- [4] P.W. Anderson, *Science* **268**, 1154 (1995).
- [5] P.W. Anderson, *Science* **279**, 1196 (1998).
- [6] A.J. Leggett, *Science* **274**, 587 (1996).
- [7] A.J. Leggett, *Science* **279**, 1157 (1998).
- [8] S. Chakravarty, cond-mat/9801025 [*Eur. Phys. J. B* (to be published)]. There is a factor of 2 difference between the estimates of Chakravarty and Anderson for λ_{ILT} .
- [9] S. Uchida, K. Tamasaku, and S. Tajima, *Phys. Rev. B* **53**, 14558 (1996).
- [10] J. Schützmann *et al.*, *Phys. Rev. B* **55**, 11118 (1997).
- [11] K.A. Moler *et al.*, *Science* **279**, 1193 (1998).
- [12] A. Tsvetkov *et al.*, *Nature* (London) (to be published).
- [13] C. Panagopoulos *et al.*, *Phys. Rev. Lett.* **79**, 2320 (1997).
- [14] D. Pelloquin *et al.*, *Physica* (Amsterdam) **273C**, 205 (1997).
- [15] D. Pelloquin, M. Hervieu, and B. Raveau (to be published).
- [16] J.R. Kirtley *et al.*, *Appl. Phys. Lett.* **66**, 1138 (1995).
- [17] J.R. Kirtley, V.G. Kogan, J.R. Clem, and K.A. Moler (to be published).
- [18] B. Billon, M. Charalambous, O. Riou, J. Chaussy, and D. Pelloquin, *Phys. Rev. B* **56**, 10824 (1997); M. Charalambous (private communication).
- [19] W.E. Lawrence and S. Doniach, in *Proceedings of the 12th International Conference on Low Temperature Physics*, edited by E. Kanda (Academic Press, Kyoto, 1971), p. 361.
- [20] L.N. Bulaevski, *Sov. Phys. JETP* **37**, 1133 (1973).
- [21] V. Ambegaokar and A. Baratoff, *Phys. Rev. Lett.* **10**, 486 (1963); **11**, 104(E) (1963).
- [22] John R. Clem and Mark W. Coffey, *Phys. Rev. B* **42**, 6209 (1990).
- [23] M.J. Graf, D. Rainer, and J.A. Sauls, *Phys. Rev. B* **47**, 12089 (1993).
- [24] A.G. Rojo and K. Levin, *Phys. Rev. B* **48**, 16861 (1993).
- [25] P.J. Hirschfeld, S.M. Quinlan, and D.J. Scalapino, *Phys. Rev. B* **55**, 12742 (1997).
- [26] V. Hardy *et al.*, *Phys. Rev. B* **56**, 130 (1997).
- [27] H.C. Montgomery, *J. Appl. Phys.* **42**, 2971 (1970).
- [28] N.E. Hussey, *et al.*, *Phys. Rev. B* **56**, R11423 (1997).
- [29] D.N. Basov, *et al.*, *Phys. Rev. B* **50**, 3511 (1994).